



This is a repository copy of *Glacial and periglacial floodplain sediments regulate hydrologic transfer of reactive iron to a high arctic fjord.*

White Rose Research Online URL for this paper:  
<http://eprints.whiterose.ac.uk/93419/>

Version: Accepted Version

---

**Article:**

Hodson, A., Nowak, A. and Christiansen, H. (2016) Glacial and periglacial floodplain sediments regulate hydrologic transfer of reactive iron to a high arctic fjord. *Hydrological Processes*. ISSN 0885-6087

<https://doi.org/10.1002/hyp.10701>

---

This is the peer reviewed version of the following article: Hodson, A., Nowak, A., and Christiansen, H. (2015) Glacial and periglacial floodplain sediments regulate hydrologic transfer of reactive iron to a high arctic fjord. *Hydrol. Process*, which has been published in final form at <https://dx.doi.org/10.1002/hyp.10701>. This article may be used for non-commercial purposes in accordance with Wiley Terms and Conditions for Self-Archiving (<http://olabout.wiley.com/WileyCDA/Section/id-820227.html>).

**Reuse**

Unless indicated otherwise, fulltext items are protected by copyright with all rights reserved. The copyright exception in section 29 of the Copyright, Designs and Patents Act 1988 allows the making of a single copy solely for the purpose of non-commercial research or private study within the limits of fair dealing. The publisher or other rights-holder may allow further reproduction and re-use of this version - refer to the White Rose Research Online record for this item. Where records identify the publisher as the copyright holder, users can verify any specific terms of use on the publisher's website.

**Takedown**

If you consider content in White Rose Research Online to be in breach of UK law, please notify us by emailing [eprints@whiterose.ac.uk](mailto:eprints@whiterose.ac.uk) including the URL of the record and the reason for the withdrawal request.



[eprints@whiterose.ac.uk](mailto:eprints@whiterose.ac.uk)  
<https://eprints.whiterose.ac.uk/>

# Glacial and periglacial floodplain sediments regulate hydrologic transfer of reactive iron to a high Arctic fjord

Andrew Hodson<sup>1,2</sup>, Aga Nowak<sup>1</sup> and Hanne Christiansen<sup>2</sup>

- 1) Department of Geography, University of Sheffield, S10 2TN, UK
- 2) Arctic Geology, University Centre in Svalbard (UNIS), P.O. Box 156, N-9171 Longyearbyen, Norway
- 3)

**Running Head:** Arctic floodplain iron transfer

This article has been accepted for publication and undergone full peer review but has not been through the copyediting, typesetting, pagination and proofreading process, which may lead to differences between this version and the Version of Record. Please cite this article as doi: 10.1002/hyp.10701

## Abstract

The transport of reactive iron (i.e. colloidal and dissolved) by a glacier-fed stream system draining a high relief periglacial landscape in the high Arctic archipelago of Svalbard is described. A negative, non-linear relationship between discharge and iron concentration is found, indicative of increased iron acquisition along baseflow pathways. Since the glaciers are cold-based and there are no intra- or sub-permafrost groundwater springs, baseflow is principally supplied by the active layer and the colluvial and alluvial sediments in the lower valley. Collectively, these environments increase the flux of iron in the stream by 40 % over a floodplain length of just 8 km, resulting in  $6 \text{ kg Fe km}^{-2}\text{a}^{-1}$  of reactive iron export for a 20% glacierised watershed. We show that pyrite oxidation in shallow-groundwater flowpaths of the floodplain is the most important source of reactive iron, although it is far less influential in the upper parts of the catchment where other sources are significant (including ironstone and secondary oxide coatings). Microbial catalysis of the pyrite oxidation occurs in the floodplain, enabling rapid, hyporheic water exchange to enhance the iron fluxes at high discharge and cause the non-linear relationship between discharge and reactive iron concentrations. Furthermore, since the pyrite oxidation is tightly coupled to carbonate and silicate mineral weathering, other nutrients such as base cations and silica are also released to the stream system. Our work therefore shows that high Arctic floodplains should be regarded as critically important regulators of terrestrial nutrient fluxes to coastal ecosystems from glacial and periglacial sources.

## Keywords

Iron fluxes; Permafrost biogeochemistry; Glacial runoff; Arctic floodplains

## Introduction

Iron cycling in glacial environments is presently receiving much research attention on account of the potential for climate change to enhance iron fluxes into an often iron-limited ocean ecosystem. In the Gulf of Alaska, clear links between glacier-fed rivers and iron availability to marine ecosystems have been identified in spite of rapid rates of removal in estuarine mixing zones (e.g. Schroth et al, 2011, 2014). The Southern Ocean also represents a compelling example of how glacial sediment inputs help alleviate iron limitation of marine primary production (Gerringa et al, 2012; Korb et al, 2008). Finally, researchers in Greenland have been making a similar case for the fertilisation potential of the ice sheet in the North Atlantic area (Bhatia et al, 2013; Statham et al, 2008; Hawkings et al, 2014), although the potential impact of these inputs upon primary production in the North Atlantic has been questioned (Hopwood et al, 2015). In the latter case, and also with Gerringa et al's (2012) work in the vicinity of Pine Island Glacier, Antarctica, great emphasis has been given to the importance of subglacial weathering environments on account of the high rock-water contact they offer, as well as the high rate of erosion that enables subglacial meltwaters to deliver the iron to downstream ecosystems. In this work, acquisition of labile iron from reactive micro-particles (colloids and nano-particles) and fine suspended sediment have been found to be quantitatively more important than "aqueous" or dissolved iron (i.e.  $< 0.02 \mu\text{m}$  following Raiswell and Canfield (2012)), and the great abundance of these particles in bulk glacial meltwater means that global glacial runoff might produce fluxes equivalent to, or greater than, icebergs and dust (Hawkings et al, 2014; Raiswell et al, 2006). Glacial runoff is therefore a potentially important vector for reactive iron delivery into the world's oceans and its sensitivity to climate change means it requires significant research consideration.

During deglaciation, the importance of iron acquisition via in-situ subglacial weathering diminishes once ice extent has declined markedly. In Svalbard and other parts of the Arctic, this is exacerbated by the fact that smaller valley glaciers also respond to mass balance losses by becoming thinner and thus no longer capable of inducing pressure melting at their base. The glacier then freezes to its substrate and surface meltwaters predominantly follow surface channels which offer almost no opportunities for rock-water contact until they become deeply incised in the ablation area by fluvial and thermal erosion (Gulley et al, 2009). Even here, the high flushing rates and channelized (rather than distributed) nature of the flows greatly restrict the opportunities for solute acquisition from sediments (Tranter et al, 1996). The onset of basal freezing therefore has very important implications for the acquisition and transport of lithogenic nutrients by meltwaters (Hodson et al, 2004), making reactive fine sediments in proglacial and periglacial environments increasingly important regulators of biogeochemical processes on account of the significant rock/water contact opportunities they offer (Nowak and Hodson, 2014a; Rutter et al, 2011). So far, these processes are best understood in the contexts of ecological succession in the soils and lakes of mid-latitude glacier forefields (e.g. Engstrom et al, 2000; Bernasconi et al, 2011), although there is also a rapidly growing, significant interest in the in-stream ecology of glacier-fed rivers (Brown et al, 2012 and references therein). However, few studies have considered in-situ hyporheic and groundwater biogeochemistry in proglacial floodplains (e.g. Gooseff et al, 2013), especially

in the context of iron. This is an important oversight, because reactive, fine sediments delivered to floodplains by glacial and periglacial processes directly interact with the large fluxes of dilute runoff that are produced during deglaciation (Milner et al, 2009). Studies of floodplain biogeochemistry in glacier-fed river systems are also best known from alpine or boreal environments, such as the European Alps (e.g. Tockner et al, 2002; Freimann et al, 2013), Alaska (Clilverd et al, 2008; Hood and Berner, 2009) and Iceland (Gislason et al, 1996; Robinson et al, 2009). However, High Arctic proglacial floodplains deserve as much, if not more, attention on account of their proximity to coastal ecosystems that are also responding to rapid sea ice changes (Arrigo et al, 2008).

In Arctic Svalbard, the location of the present study, important contributions to our understanding of biogeochemical cycling downstream of glacier margins are largely restricted to the immediate glacier forefield, and usually within recent end moraines from the Little Ice Age (or glacier surge activity) (e.g. Ansari et al, 2013; Cooper et al, 2002; Wadham et al, 2007). However, Nowak and Hodson (2014a,b) have argued that downstream microbial ecosystems within the proglacial floodplains are very productive and contribute significantly to watershed solute fluxes via reactions that are not unlike subglacial weathering processes. Similarly, Ansari et al (2013) and Nowak and Hodson (2014b) have shown here that periglacial processes can be just as important as glacial processes in the provision of reactive crushed rock surfaces for microbially-mediated weathering. Work conducted on the Svalbard archipelago has also emphasised the geomorphological and hydrological importance of floodplains and alluvial sediments, especially near the coast (Strzelecki et al, 2014). Since the Last Glacial maximum, vast sediment packages have been deposited here by glacio-marine sedimentation prior to isostatic uplift and permafrost aggradation, and resulting in major floodplains in all fjords no longer dominated by calving glacier margins (Etzelmüller and Hagen, 2005). Glacier retreat since the Little Ice Age maximum of the early 1900s has also occurred at a rate of ca. 0.3% per year (Nuth et al, 2007), which is having a profound effect upon the exposure of young glacial sediments and their mobilisation into the floodplains and coastal fans by contemporary runoff. For example, Strzelecki et al (2014) estimated an average net accumulation rate of ca. 5.5 cm a<sup>-1</sup> across the outwash plains, deltas and tidal flats in Northern Petuniabukta, Central Spitsbergen.

The objective of this paper, therefore, is to provide much-needed insights into the seasonal dynamics of reactive iron (hereafter \*Fe, defined as all dissolved and colloidal iron that passed through 0.45µm filter) and its transport through a High Arctic floodplain system. In so doing we examine a lowland glacier-fed river and compare ice-marginal \*Fe dynamics to those downstream and within a near-coastal sediment fan.

### **Field Site Description**

The fieldwork was conducted in the Endalen watershed adjacent to Longyearbyen in Svalbard (Figure 1). The catchment supplies runoff produced by glacial meltwater, active layer thaw, snowmelt and rain to Isdammen, the artificial lake providing winter water supply to the local town of Longyearbyen. During summer, the runoff is used to fill the lake and then overflows into Adventfjord. The catchment is ca. 28 km<sup>2</sup>, of which ca. 16% is covered by

permanent glacier ice, with one larger glacier, Bogerbreen (ca. 3.3 km<sup>2</sup>), occupying the upper part of the valley. The mountains that flank the valley are ca. 500m high plateaus, and so only small residual snowbanks and a couple of un-named cirque glaciers (Figure 1) sustain flows all summer, because the snowline often retreats to elevations in excess of 600 m. By the end of July, therefore, Bogerbreen in fact produces the vast majority of discharge. This is a typical small valley glacier for this region, and so while the presence of striae in the glacier's terminal moraines attest to the presence of warm basal ice during the Little Ice Age maximum (when the moraines were most likely deposited), a century or so of thinning means that the glacier is now almost certainly cold-based with no evidence of subglacial drainage or temperate ice at the pressure melting point (Macheret and Zhuravlev, 1982). This shift toward cold-based glaciation over recent decades is almost certainly commonplace in the region, as revealed by several detailed case studies linking the mass balance, climate and thermal regime change in local glaciers (Bælum and Benn, 2011; and Hodgkins, 1999). Furthermore, there is a canyon at the immediate margin of its Little Ice Age moraines. Water storage in the upper part of the catchment is therefore greatly reduced by both the cold-based glacier and the canyon, such that most surface waters are transferred rapidly to the lower valley floodplain. Here, snowmelt, ground ice melt, rain and cirque glacier melt percolate through colluvial and alluvial fans, talus deposits and solifluction sheets before mixing with runoff from Bogerbreen (Fig. 1). Collectively, they enter a large alluvial sediment fan that is accumulating in the mouth of the Endalen.

The lithology of the catchment is dominated by sedimentary rocks (sandstones, shales and carbonates), that belong to the well-known van Mijenfjord and Adventdalen Groups and include some very reactive mineral phases such as carbonate and pyrite (Dallman et al, 1999). Studies of runoff geochemistry in the area have so far neglected the geochemistry of iron, but otherwise describe well how these minerals contribute to the composition of runoff (see Yde et al, 2008; Rutter et al, 2011). The rock sequences are well-known on account of their coal content and belong to the Firkanten, Basilika and Grumantbyen Formations of the Paleocene, and the Frysjaodden, Hollenderdalen, Battfjellet and Aspelintoppen Formations of the Eocene (Dallmann et al, 1999). Iron is present as pyrite, siderite and glauconite in the sandstones (Svinth, 2013), and shales (especially in the Frysjaodden) (Riber, 2009). Minor sources of iron also include biotite and chlorite (chamosite). The Firkanten Formation holds the most commercially viable coal seam, which was the reason for the opening of a coal mine in Endalen. Although the mine is no longer operational, some of the waste rocks just upstream of the valley mouth are now subjected to chemical weathering by surface waters. Sediment inputs from here represent a small supplement to the overwhelming natural supply of crushed rock to the river by glacial, periglacial and fluvial processes. The relict mine is also dry, and no related groundwater discharges were observable during summer or winter. Therefore seasonal rock-water contact in the mine tailings within the active layer only occurs in valley side during snowmelt and rain in summer.

The geology and the geomorphic processes in Endalen are conducive to high sediment yields (Bogen and Bønsnes, 2003) and so there has been a lot of sedimentation in the large alluvial fan of the lower valley. Following the Last Glacial Maximum, plateau glaciers also delivered

large volumes of sediment along the flanks of the main valley (Soltvedt, 2000) to produce numerous smaller fans. These are now stable with the exception of small-scale debris flows, which occur following the loading of the valley sides and plateaus by snow. The largest fan at the valley mouth enters Adventdalen, upstream of the artificial lake “Isdammen” (Figure 1). Early aerial photographs clearly show that the fan existed long before Isdammen was constructed, and that the waterflow was diverted towards the Isdammen area by a natural barrier existing to the north (Fig. 1). Further, raised beaches at 36, 50, 57 and 63 m altitude in the lower valley show that the lower part of Endalen lies within the former marine limit. Therefore marine sediment sequences exist just beneath the lower floodplain and fan sediments (Gilbert, 2014). These were formed rapidly following the retreat of the Weichselian Ice Sheet from the inner fjord about 10 000 years ago (Lønne and Nemec, 2004; Soltvedt, 2000).

## Methods

River monitoring stations were installed at three locations shown in Figure 1. Here hourly records of river runoff, electrical conductance (“EC”) and water temperature were collected over the 2012 melt season with the use of Campbell data loggers and compatible sensors (see Table 1). Data records from the upper Endalen site (hereafter “EU”) were shorter than other locations due to access issues in the early summer. However, despite that, samples from here were still sufficient for characterising glacial water and solute inputs to the valley system. Further downstream, the Lower Endalen site (hereafter “EL”) and the Isdammen inflow site (hereafter “ISD”) were used to represent processes within the lower valley and the alluvial fan at the valley mouth. Measurements of water stage were calibrated to discharge using the salt dilution method (Moore, 2005), which was conducted every time samples were collected at the stations. Errors with this technique are typically 10% (e.g. Hodson et al, 2000). Discharge records from EL were also used to represent ISD, because there were no significant water inputs between these sites and an average transit time between them of just 1 h according to cross correlation analysis.

Suspended sediment transport monitoring was conducted using automatic pump samplers at Sites EL and ISD for the duration of the summer. In addition, suspended sediment concentration was also determined at all three sites from the filter papers used during the collection of each water quality hand sample. The Sigma Automatic Pump Samplers were programmed to collect 500 mL samples three times a day and these were then filtered at UNIS in the same manner as the other water quality samples (see below).

Samples for the determination of major ions and trace metals were collected at frequent intervals (see Table 1 for details) using a pre-rinsed 250 mL HDPE bottle. During the sampling, the pH of the water was also recorded using a daily calibrated VWR handheld pH meter. Back at UNIS, samples were immediately filtered through a Whatman Cellulose Nitrate (WCN) 0.45  $\mu\text{m}$  filter using a pre-rinsed 500ml Nalgene filtration unit. All samples for major ions and dissolved Si (a subset of which is presented in the present paper) were then stored at 4 °C with no air for up to three months until the analyses in the UK. Additionally, samples collected for trace metals analyses were acidified with high purity

HNO<sub>3</sub> (AnalaR 65% Normapur, VWR, IL, USA) to pH ~ 2. These were stored at 4 °C in 15 mL, acid-washed Eppendorf tubes after further rinsing four times with filtrate.

### Laboratory analysis

Laboratory analyses involved the determination of dissolved Silica (Si) by colorimetric methods (using a Skalar SAN++ continuous flow analyser), major ions by ion chromatography (with the use of Dionex ion chromatograph (DX 90, operated through a 4400 integrator and AS40 autosampler) and trace metals by Inductively Coupled Plasma Mass Spectrometry (PerkinElmer Elan DRC II, MA, USA). Precision errors for all the analyses were below 5% and the detection limit was 1.0 µg L<sup>-1</sup>. No contaminants above this limit were detected in the analyses of blank samples.

## Results

### Time Series Observations

Hydrological time series, including discharge, EC and suspended sediment concentrations (SSC) are presented in Figure 2. Widespread snowmelt runoff in the catchment peaked at around Day of Year (hereafter DOY) 175 and was responsible for the beginning of the season maximum in river discharge at EL and ISD. Additionally, high river flows were also observed around DOYs 198, 205 and 223, with the first two being a consequence of relatively high rainfall. End of season low flows resulted from a flow recession that commenced on DOY 223 and persisted until the end of monitoring. During the part of the observation period when records were available at all river monitoring sites (i.e. the DOY 196 onwards), the ratio of discharge at EU to that recorded at EL was 76% (defined using the slope of a linear regression model between the two series, with an  $r^2$  of 0.86 and a significance level  $\leq 0.02$ ). The relationship between discharge at EU and EL was also characterised by a lag of 5 hours and a significant ( $p \leq 0.05$ ) intercept of 0.095 m<sup>3</sup> sec<sup>-1</sup>, indicating a downstream input of water that is equivalent to 20% of the average flow at EU. Figure 2 also shows that the high flow phases described above caused dilution in the ionic content of runoff at all three sites and thus an inverse relationship between discharge and EC. Further, during the low flow phases (around DOY 180 and after DOY 235), high values of EC were observed at all sites.

Figure 3 shows that concentrations of \*Fe varied significantly (10 – 520 µg L<sup>-1</sup>) through the summer. Before DOY 234, \*Fe concentrations were typically greatest at ISD, although there were exceptions when samples coincided with the rising limb of discharge during periods of high flow when they were greatest at EU and EL (e.g. DOYs 196 and 202). After DOY 232, \*Fe concentrations were marginally lower at ISD than EL, implying removal during low flow conditions. The \*Fe fluctuations were therefore broadly similar to EC, with the exception of the seasonal maximum \*Fe levels observed during early summer at EL and ISD prior to DOY 168 (there are insufficient data to assess whether this was also the case at EU). Later on, the end of season increase in \*Fe concentrations was a significant feature at all the sites and therefore demonstrated similar behaviour to the EC variations. The pH values for runoff are also presented in Figure 3 and can be seen to lie in the typical range for glacial catchments,

between 5.8 and 8.0. The pH generally increased throughout the summer at all sites, but there were some short term pH depressions around DOYs 176, 195 and 216.

Suspended sediment concentrations are shown in Figure 2. There are several key features to the data: first the SSC generally increased at ISD (at least until DOY 223) and second, the SSC at ISD was less variable than at EL, and typically exceeded concentrations at EL after DOY 223. Otherwise, maximum SSCs were associated with rainfall-induced high flows between DOY 185 and 209.

#### Water, \*Fe and SSC Flux Estimates

\*Fe fluxes were estimated from the product of the discharge-weighted mean \*Fe concentration and the estimated total annual runoff at each site (Table 2). The annual runoff volume was assumed to be 90 times the average daily discharge at each site, and therefore assumes a 90 day runoff season. This implies no significant flows occurred outside the period DOY 150 - 240. The likelihood is that rainfall events after DOY 240 triggered sporadic river flows (and thus reactive iron transfer) (e.g. Nowak and Hodson, 2013). However, we lack the data to quantify such events. Conservative estimates of the errors for the flux calculations, based upon Hodson et al's (2000) study of Svalbard solute fluxes, were 24.5% and 19.4% at EL and ISD respectively, but as much as 48.3% at EU. The high error estimate at EU was due to the low number of observations ( $n = 8$ ) and its effect upon the standard error of the mean.

Since the SSC records covered almost the entire summer period without bias (e.g. to high flows), the total annual suspended sediment transfer was estimated from suspended sediment load estimates at EL and ISD that were calculated from the product of river discharge and SSC. The average load was then scaled to estimate total fluxes for the same periods of interest as the \*Fe fluxes and with an uncertainty estimate of 16% at both sites (i.e. EL and ISD). The values were then transformed to a suspended sediment yield (in  $\text{t km}^{-2}$ ) after dividing by catchment area (Table 2).

Table 2 shows that specific runoff decreased downstream, as might be expected for a glacier-fed system that is dominated by a larger glacier at high elevation. Overall the entire watershed's specific runoff was 0.23 m during 2012. This is low compared to the range ( $0.35 - 1.5 \text{ m a}^{-1}$ ) presented for Svalbard watersheds by Hodson et al (2000), although it should be noted that the Endalen watershed has only 16% glacier cover and most of the studies in the literature are for basins with in excess of 50% glacier cover. Unsurprisingly, the suspended sediment yield in the present study ( $136$  and  $114 \text{ t km}^{-2}$  at EL and ISD respectively) is also low for Svalbard studies and lies at the lower end of the range of values recorded at ISD by previous researchers (i.e.  $134 - 568 \text{ t km}^{-2}$  according to Bøgen and Bosnes, 2003). Table 2 also shows how the second half of the summer period (DOY 195 to 240) was the most effective period for suspended sediment export from the entire watershed. Therefore the (45 day) DOY 195 - 240 yield at ISD ( $79.6 \text{ tons km}^{-2}$ ) was 67 % of the entire (90 day) DOY 150 - 240 yield ( $114 \text{ t km}^{-2}$ ). However, the corresponding \*Fe yields did not show this bias, and were ca.  $6 \text{ kg km}^{-2}$  for the entire 90 day period at EL and ISD respectively. Just less than half

of this was supplied in the latter half of the summer (DOY 195 – 240), which was in broad agreement with the temporal distribution of runoff (see Table 2).

## Discussion

### \*Fe concentrations and fluxes in the Endalen valley

The discharge-weighted average \*Fe concentrations at EU, EL and Isd were 27.3, 24.5 and 23.6  $\mu\text{g L}^{-1}$  respectively (Table 2). These values are more than 300 times higher than that which would be expected from the solubility of ferrihydrite under the conditions described in the Endalen river (Kraemer, 2004). They also exceed \*Fe concentrations in meltwaters draining a small cold-based glacier upon metamorphic rocks in the maritime Antarctic (3.43  $\mu\text{g L}^{-1}$ ; Hodson et al, 2010) and a couple of minor outlet glaciers overlying crystalline bedrock and flowing from the Greenland Ice Sheet (1.12 – 9.88  $\mu\text{g L}^{-1}$ ; Statham et al, 2008). The differences here might therefore relate to the presence of reactive sedimentary rocks in the present study. The range of reactive iron concentrations in the present study (10 – 520  $\mu\text{g L}^{-1}$ ; see Figure 4) also exceeds that of a subglacial river draining a different outlet glacier from the Greenland Ice Sheet (13 – 260  $\mu\text{g L}^{-1}$ ; Hawkings et al, 2014), and both glacial meltwaters and shallow groundwaters draining Mittivakkat Glacier, Greenland (56 – 90  $\mu\text{g L}^{-1}$ ; Kristiansen et al, 2013). It does however compare favourably with subglacial waters of an Alpine glacier where metamorphic rocks are present (15 – 1,200  $\mu\text{g L}^{-1}$ ; Mitchell et al, 2001).

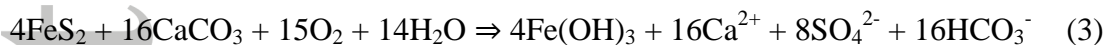
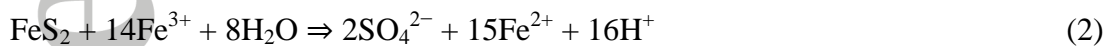
Figure 4 presents the relationship between catchment outflow (discharge) and \*Fe concentrations at EL, showing that discharge was most enriched in \*Fe at low, baseflow-dominant conditions. The result is a significant, negative correlation between \*Fe and the natural logarithm of discharge (Pearson's correlation coefficient  $r = 0.81$ ,  $p \leq 0.05$ ). Figure 4 also suggests that \*Fe acquisition was maintained at high flows by rapid acquisition, which suppressed the effect of dilution and thus made the relationship non-linear. Such a relationship was absent at EU ( $r = 0.28$ ,  $p > 0.05$ ), indicating a weak hydrological control upon \*Fe concentrations in the upper catchment. Furthermore, no statistically significant ( $p \leq 0.05$ ) correlations between \*Fe and suspended sediment concentration could be found at any of the sites using estimates of the latter derived from either hand sampling or automatic pump sampling. Therefore, whilst \*Fe fluxes increase with discharge, concentrations do not, and so they behave more like solutes than suspended sediment (see also Figure 2). The relevant mechanisms by which runoff acquires \*Fe are therefore sought below.

### \*Fe acquisition by runoff

The apparent “excess” of \*Fe in surface waters (relative to the expected dissolved concentrations at thermodynamic equilibrium in the Endalen stream) and the marked importance of \*Fe acquisition by baseflow in the lower valley can be attributed to either: 1) an influx of aqueous  $\text{Fe}^{2+}$  via anoxic groundwater inflow; and/or 2) inputs of iron microparticles or colloids, such as ferric oxyhydroxides or perhaps Schwertmannite (Raiswell et al, 2009), supplied by weathering. We can assert with confidence that there are no anoxic ferrous inflows associated with perennial groundwater springs, because we have been systematically mapping all such springs in the region since 2011 as part of a study of intra-

and sub-permafrost groundwater (Nowak and Hodson, Unpublished Data). However, anoxic, ferrous springs could develop seasonally in saturated sediments of the lower floodplain, as was witnessed for part of the 2012 summer in the vicinity of the mine tailings immediately upstream of EL where both Schwertmannite and ferrihydrite precipitation were visible in small areas. However, the small spring at the base of the mine tailings here was far too insignificant to explain the abundance of \*Fe in the otherwise natural system. Therefore, \*Fe acquisition by weathering in natural weathering environments is considered below.

Figure 4 shows very strong relationships between \*Fe, SO<sub>4</sub><sup>2-</sup> and Ca<sup>2+</sup> ions, especially during late summer, baseflow-dominant conditions, when the importance of rock-water contact in the floodplain sediments was maximised at EL and ISD. These data strongly suggest that pyrite oxidation (Equation 1 and 2) coupled to carbonate dissolution (Equation 3) were the dominant processes governing \*Fe, Ca<sup>2+</sup> and SO<sub>4</sub><sup>2-</sup> acquisition in the floodplain. The strong association between \*Fe and SO<sub>4</sub><sup>2-</sup> was most pronounced during the flow recession (after DOY 223), when the relationship was highly statistically significant at both EL and ISD ( $p \leq 0.01$ ;  $r^2 = 0.99$ ). Furthermore, the relationship between these parameters was similar ( $p < 0.03$ ;  $r^2 = 0.92$ ) when all data from both EL and ISD after DOY 155 were considered. The strong relationship between \*SO<sub>4</sub><sup>2-</sup> and Ca<sup>2+</sup> also occupies an identical domain on the graph to data from the nearby Bolterdalen and Longyeardalen catchments (after Rutter et al, 2011 and Yde et al. 2007, respectively: data not shown). This demonstrates the regional importance of pyrite oxidation and carbonate weathering, which we have now shown to include the acquisition of \*Fe from floodplain sediments as well.



The kinetics of microbially mediated pyrite oxidation in glacial sediments are known to enable far more rapid acquisition of SO<sub>4</sub><sup>2-</sup> (and thus by implication \*Fe) from glacial sediments than abiotic oxidation (Raiswell and Canfield, 2012). The dominance of microbially-mediated sulphide oxidation in this environment is also well established from stable isotope analyses (e.g. Bottrell and Tranter, 2002; Hodson et al, 2010; Wynn et al, 2006) and studies of major ion concentrations elsewhere in the region (e.g. Cooper et al, 2002; Nowak and Hodson, 2014a,b). Therefore rapid \*Fe acquisition from the floodplain sediments in closest proximity to the channel (i.e. the hyporheic zone) by microbially mediated sulphide oxidation, followed by their transportation as Fe(OH)<sub>3</sub> microparticles in the stream, is the best explanation for the non-linear association between discharge and \*Fe shown in Figure 4 (because rapid acquisition is necessary at higher flows to cause the non-linearity). The process is therefore responsible for much of the large increase (40%) in the \*Fe flux from EU to ISD that is shown by Table 2, because the \*Fe flux increased with discharge. To our knowledge, this is the first data set that demonstrates the tight coupling between \*Fe and sulphide oxidation in proglacial stream systems, which is surprising given

that the importance of pyrite oxidation as a source of  $\text{SO}_4^{2-}$  to glacial runoff was first described by Raiswell (1984) some thirty years ago.

Nowak and Hodson (2014a) showed that microbially-mediated sulphide oxidation is also likely to be coupled to silicate mineral weathering in glacial floodplains. Unsurprisingly, Figure 4 also indicates strong relationships between Fe,  $\text{SO}_4^{2-}$  and Si at EL and ISD which further support this observation. However, Figure 4 reveals that while statistically significant associations between \*Fe and both  $\text{SO}_4^{2-}$  and Si were observed at EL and ISD, they were not apparent at EU. Therefore, since the \*  $\text{SO}_4^{2-}$  concentrations were also relatively low at EU, far less \*Fe and Si acquisition may be attributed to pyrite oxidation in the upper parts of the watershed, and other sources of \*Fe need to be invoked. The same is the case for the first five days of the sampling period (i.e. prior to DOY 156) at EL and ISD, because far greater \*Fe concentrations occurred for the given  $\text{SO}_4^{2-}$ . Other sources of \*Fe were therefore sought for these instances. However, no statistically significant ( $p \leq 0.05$ ) relationships among \*Fe, Si and  $\text{Al}^{3+}$  were found (data not shown), making (alumino)silicate mineral weathering an unlikely source of the additional \*Fe. Secondly, the relationship between \*Fe and  $\text{HCO}_3^-$  was very poorly defined at all three sites ( $p > 0.10$ ), suggesting that the siderite can also perhaps be discounted. This leaves \*Fe oxides associated with the ironstones or potential secondary precipitates (visible as iron-staining on the surface of many gravel clasts in the valley) as the most obvious remaining sources. Testing their importance using statistical relationships among solute data was not possible. However, we note that snowmelt-driven overland flow was observable when the early summer high \*Fe values were reported at EL and ISD (ie prior to DOY 156). Therefore we hypothesise that the mobilisation of secondary  $\text{Fe}_{\text{III}}$  precipitates from the surface of the catchment is potentially important before significant active layer development during the early stages of summer.

#### Iron vs suspended sediment fluxes and yields

Although we found no correlation between \*Fe and SSC, research has shown how operationally defined extractions remove a large pool of potentially labile iron from the surface of glacial rock flour (Hawkings et al, 2014; Hopwood et al, 2014; Mitchell et al, 2001; Schroth et al, 2011,2014). Even though the extractions were not carried out here, the high suspended sediment yields (Table 2) almost certainly mean that they transported a significant extractable iron flux downstream. The dynamics of sediment-bound labile Fe and \*Fe were likely to have been quite different in the present study. For example, a small proportion (13 %) of suspended sediment was stored in the fan between EL and ISD, whilst according to Table 2, the fan acted as a net source (17%) of \*Fe between these two points over the course of the entire summer. Further, the suspended sediment transport dynamics in the Endalen valley showed no evidence of seasonal exhaustion, as is often the case when subglacial erosion dominates glaciofluvial sediment transport (e.g. Figure 2 in Hawkings et al, 2014), especially in Svalbard (Hodson and Ferguson, 1999). Instead, SSCs remained significant throughout the summer: a characteristic that is common for catchments with cold-based glaciers because ground thaw, rather than subglacial erosion, dominates the supply of available sediment to the stream (Hodgkins, 1996, Hodson and Ferguson, 1999). In addition, suspended sediment transport in Endalen was also enhanced by several significant rainfall

events throughout the summer (data not shown). As a consequence, Table 2 shows that while the second half of the observation period produced 52% of the total runoff volume and \*Fe flux, it accounted for 64% of the suspended sediment flux, indicative of increased suspended sediment availability as summer progressed. Therefore the dynamics of labile, sediment-bound iron associated with suspended sediment are not likely to be uniform from one type of glacial system to another, and so we caution against the uncritical up-scaling of flux data from just a few locations until more research has been undertaken.

\*Fe immobilisation in the lower fan?

The potential immobilisation of \*Fe and  $\text{SO}_4^{2-}$  was detectable as a decrease in concentrations of both parameters between EL and ISD during the lowest flows after DOY 234. At this time, the decline in concentrations of \*Fe and  $\text{SO}_4^{2-}$  between EL and ISD were highly correlated ( $p < 0.05$ ;  $r = 0.94$  and  $n = 6$ ), suggesting that removal by sulphate reduction and pyrite precipitation might be occurring following hyporheic water exchanges between the very slow moving stream (at low flow) and the sediments of the lower fan. Removal processes have also been inferred by changes in Fe concentrations (but not fluxes) at three points along the alluvial plain in front of Austre and Vestre Brøggerbreen glaciers by Zhang et al (2015). The slope of relationship between the concentration changes was equivalent to one mole of \*Fe for every 1.3 moles of  $\text{SO}_4^{2-}$ , which suggests a mixture of FeS and FeS<sub>2</sub> precipitation, or perhaps FeS and elemental sulphur (Bottrell et al, 1995; Schoonen, 2004), rather than removal by FeS<sub>2</sub> alone (since this would produce a net molar ratio of two). Apart from low temperatures, a major reason for this effect not being more apparent is most likely the lack of organic matter in the floodplain sediments (Raiswell and Canfield, 2012), as has also been inferred from the pore water and sediment geochemistries of fjord sediment cores from close proximity to glaciers in Svalbard (Wehrman et al, 2014) and the maritime Antarctic (Monien et al, 2014). A most interesting speculation, therefore, is whether the stabilisation of the floodplain environment by vegetation (that usually follows deglaciation: Milner et al, 2009), will result in quantitatively more important rates of pyrite precipitation, resulting in a switch towards net iron storage within the floodplain. Similarly, hydrologic changes associated with a deeper, more persistent active layer during the summer might lead to extended residence times within the hyporheic zone and also serve to enhance the \*Fe removal processes. Further research into the long-term biogeochemical evolution of high Arctic floodplains is therefore required.

## Conclusions

Our study shows that central Svalbard's Tertiary Basin is characterised by easily eroded, chemically reactive sedimentary rocks that produce a hotspot of reactive iron production for mobilisation by hydrologic processes. Deglaciation of this landscape means that meltwaters rework vast packages of fine glacial sediments from catchment headwaters to downstream floodplains: a process that continues whilst smaller valley glaciers undergo a transition to cold-based thermal regime and then eventually disappear. As a consequence downstream floodplain and other periglacial sediment deposits become the most important crushed rock reactors at the expense of subglacial environments. It is becoming increasingly obvious in Svalbard that this has important implications for nutrient transfer to the sea, as has been argued for phosphorus (Hodson et al, 2004), nitrogen (Ansari et al, 2013) and a wide range of mineral weathering products (Nowak and Hodson, 2014a). Here we have shown that the same now applies to reactive iron. Glacial headwaters draining cold-based glaciers seem far less capable of acquiring reactive iron via pyrite oxidation than pore waters draining through talus, colluvial/alluvial debris fans and floodplain sedimentary environments. We have found that rapid, microbially-mediated pyrite oxidation in these glacial and periglacial sediments may increase the reactive Fe flux significantly over reach scales of several kilometres from the retreating glacier margin. Periglacial biogeochemical processes therefore provide a crucial service for coastal marine ecosystems through the provision of reactive iron from sources that will most likely continue to be important long after climate change has removed the glacier from the catchment.

**Acknowledgements.** This study was funded by the Longyearbyen Lokalstyre Bydrift. The authors would like to thank Andrew Gray, Krystyna Koziol and UNIS students (members of the AG340 class of 2012) for field assistance.

Accepted

## References

- Ansari AH, Hodson AJ, Kaiser J, and Marca-Bell A. 2013. Stable isotopic evidence for nitrification and denitrification in a High Arctic glacial ecosystem. *Biogeochemistry*, **113**(1-3): 341-357. DOI: 10.1007/s10533-012-9761-9.
- Arrigo KR, van Dijken G, and Pabi S. 2008. Impact of a shrinking Arctic ice cover on marine primary production. *Geophysical Research Letters* **35**, L19603. DOI: 10.1029/2008GL035028.
- Bælum K, and Benn DI. 2011. Thermal structure and drainage system of a small valley glacier (Tellbreen, Svalbard), investigated by ground penetrating radar. *The Cryosphere* **5**(1): 139-149. DOI:10.5194/tc-5-139-2011.
- Bernasconi SM, Baude, A, Bourdon B, and 37 others. 2011. Chemical and biological gradients along the Damma glacier soil chronosequence, Switzerland. *Vadose Zone Journal* **10**(3): 867-883. DOI: 10.2136/vzj2010.0129.
- Bhatia MP, Kujawinski EB., Das SB, Breier CF, Henderson PB. and Charette MA. 2013. Greenland meltwater as a significant and potentially bioavailable source of iron to the ocean. *Nature Geoscience* **6**(4): 274-278. DOI: 10.1038/ngeo1746.
- Bogen J. and Bønsnes T. 2003. Erosion and sediment transport in High Arctic Rivers, Svalbard, *Polar Research* **22** (2): 175-189. DOI: 10.1111/j.1751-8369.2003.tb00106.x.
- Bottrell SH, and Tranter M. 2002. Sulphide oxidation under partially anoxic conditions at the bed of the Haut Glacier d'Arolla, Switzerland. *Hydrological Processes* **16**(12): 2363-2368. DOI: 10.1002/hyp.1012.
- Bottrell SH, Hayes PJ, Bannon M, and Williams GM. 1995. Bacterial sulfate reduction and pyrite formation in a polluted sand aquifer. *Geomicrobiology Journal* **13**(2): 75-90.
- Brown, LE, and Milner, AM. 2012. Rapid loss of glacial ice reveals stream community assembly processes. *Global Change Biology* **18**(7): 2195-2204. DOI: 10.1111/j.1365-2486.2012.02675.x.
- Clilverd HM, Jones Jr JB and Kielland K. 2008. Nitrogen retention in the hyporheic zone of a glacial river in interior Alaska. *Biogeochemistry* **88**(1): 31-46. DOI: 10.1007/s10533-008-9192-9.
- Cooper RJ, Wadham JL, Tranter M, Hodgkins R, and Peters, NE. 2002. Groundwater hydrochemistry in the active layer of the proglacial zone, Finsterwalderbreen, Svalbard. *Journal of Hydrology* **269**(3): 208-223. DOI: 10.1016/S0022-1694(02)00279-2.
- Dallmann WK, Midbø PS, Nøttvedt A and Steel RJ. 1999. Tertiary lithostratigraphy. In: *Lithostratigraphic Lexicon of Svalbard*, Dallmann WK. (ed). Norsk Polarinstitut: Tromsø; 215-263.
- Engstrom DR, Fritz SC, Almendinger JE, and Juggins S. 2000. Chemical and biological trends during lake evolution in recently deglaciated terrain. *Nature* **408**(6809): 161-166. DOI:10.1038/35041500.
- Etzelmüller B, and Hagen JO. 2005. Glacier-permafrost interaction in Arctic and alpine mountain environments with examples from southern Norway and Svalbard. *Geological Society, London, Special Publications* **242**(1): 11-27. DOI: 10.1144/GSL.SP.2005.242.01.02

Freimann R, Bürgmann H, Findlay SE, and Robinson, CT. 2013. Bacterial structures and ecosystem functions in glaciated floodplains: contemporary states and potential future shifts. *The ISME journal*. **7**: 2361-2373. DOI:10.1038/ismej.2013.114.

Gerringa LJ, Alderkamp AC, Laan P, Thuroczy CE, De Baar HJ, Mills MM, van Dijken GL., van Haren H. and Arrigo KR. 2012. Iron from melting glaciers fuels the phytoplankton blooms in Amundsen Sea (Southern Ocean): Iron biogeochemistry. *Deep Sea Research Part II: Topical Studies in Oceanography* **71**: 16-31. DOI: 10.1016/j.dsr2.2012.03.007.

Gilbert GL. 2014. Sedimentology and geocryology of an Arctic fjord head delta (Adventdalen, Svalbard). Unpublished University of Oslo MSc thesis, 124 p. <http://urn.nb.no/URN:NBN:no-4605>.

Gislason SR, Arnorsson S and Armannsson H. 1996. Chemical weathering of basalt in Southwest Iceland; effects of runoff, age of rocks and vegetative/glacial cover. *American Journal of Science* **296**(8): 837 – 907. DOI: 10.2475/ajs.296.8.837.

Gooseff MN, JE Barrett, and JS Levy. 2013. Shallow groundwater systems in a polar desert, McMurdo Dry Valleys, Antarctica. *Hydrogeology Journal* **21**(1): 171-183. DOI: 10.1007/s10040-012-0926-3.

Gulley JD, Benn DI, Muller D, and Luckman A. 2009. A cut-and-closure origin for englacial conduits in uncrevassed regions of polythermal glaciers. *Journal of Glaciology* **55**(189): 66–80.

Hawkings JR, Wadham JL, Tranter M, Raiswell R, Benning LG, Statham PJ, Tedstone A, Nienow P, Lee K and Telling J. 2014. Ice sheets as a significant source of highly reactive nano-particulate iron to the oceans. *Nature Communications* **5**, 3929. DOI: 10.1038/ncomms4929.

Hodgkins, R. 1996. Seasonal trend in suspended-sediment transport from an Arctic glacier, and implications for drainage-system structure. *Annals of Glaciology* **22**: 147-151.

Hodgkins R. 1999. Controls on suspended-sediment transfer at a High-Arctic glacier, determined from statistical modelling. *Earth Surface Processes and Landforms* **24**: 1–21. DOI: 10.1002/(SICI)1096-9837(199901)24:1.

Hodgkins R, Hagen JO, and Hamran SE. 1999. 20th century mass balance and thermal regime change at Scott Turnerbreen, Svalbard. *Annals of Glaciology* **28**(1): 216-220. DOI: <http://dx.doi.org/10.3189/172756499781821986>.

Hodson, AJ. and Ferguson, RI. (1999). Fluvial suspended sediment transport from cold and warm-based glaciers in Svalbard. *Earth Surface Processes And Landforms* **24**(11), 957-974. DOI:10.1002/(SICI)1096-9837(199910)24:11<957::AID-ESP19>3.0.CO;2-J.

Hodson A, Heaton T, Langford H, and Newsham K. 2010. Chemical weathering and solute export by meltwater in a maritime Antarctic glacier basin. *Biogeochemistry* **98**(1-3): 9-27. DOI:10.1007/s10533-009-9372-2.

Hodson AJ, Mumford PN and Lister D. 2004. Suspended sediment and phosphorus in proglacial rivers: bioavailability and potential impacts upon the P status of ice-marginal receiving waters. *Hydrological Processes* **18**(13): 2409 - 2422. DOI:10.1002/hyp.1471.

Hodson A, Tranter M, and Vatne, G. 2000. Contemporary rates of chemical denudation and atmospheric CO<sub>2</sub> sequestration in glacier basins: An Arctic perspective. *Earth Surface Processes and Landforms* **25**(13): 1447-1471. DOI: 10.1002/1096-9837(200012)25:13.

Hood E, and Berner L. 2009. Effects of changing glacial coverage on the physical and biogeochemical properties of coastal streams in southeastern Alaska. *Journal of Geophysical Research: Biogeosciences* (2005–2012) **114**(G3). DOI: 10.1029/2009JG000971.

Hopwood, M J, Bacon S, Arendt K, Connelly DP. and Statham PJ. 2015. Glacial meltwater from Greenland is not likely to be an important source of Fe to the North Atlantic.

*Biogeochemistry* **124**: 1-11. DOI: 10.1007/s10533-015-0091-6.

Hopwood MJ, Statham PJ, Tranter M, and Wadham JL. 2014. Glacial flours as a potential source of Fe (II) and Fe (III) to polar waters. *Biogeochemistry* **118**(1-3): 443-452. DOI: 10.1007/s10533-013-9945-y.

Korb RE, Whitehouse MJ, Atkinson A, and Thorpe SE. 2008. Magnitude and maintenance of the phytoplankton bloom at South Georgia: A naturally iron-replete environment. *Marine Ecology Progress Series* **368**, 75-91.

Kristiansen SM, Yde JC, Barcena TG, Jakobsen BH, Olsen J, and Knudsen, NT. 2013. Geochemistry of groundwater in front of a warm-based glacier in Southeast Greenland. *Geografiska Annaler: Series A, Physical Geography* **95**(2): 97-108.

DOI: 10.1111/geoa.12003.

Kraemer SM. 2004. Iron oxide dissolution and solubility in the presence of siderophores. *Aquatic sciences* **66**(1), 3-18. DOI: 10.1007/s00027-003-0690-5.

Lønne I, and Nemeč W. 2004. High-arctic fan delta recording deglaciation and environment disequilibrium. *Sedimentology* **51**(3): 553-589. DOI: 10.1111/j.1365-3091.2004.00636.x.

Milner A.M., Brown L.E. and Hannah D.M. (2009), Hydroecological response of river systems to shrinking glaciers, *Hydrological Processes* **23**, 62-77 DOI: 10.1002/hyp.7197.

Macheret Yu. Ya. and Zhuravlev, AB. 1982. Radio echo-sounding of Svalbard glaciers. *Journal of Glaciology* **28**(99), 295 – 314.

Mitchell A, Brown GH, and Fuge R. 2001. Minor and trace element export from a glacierized Alpine headwater catchment (Haut Glacier d'Arolla, Switzerland). *Hydrological Processes* **15**(18), 3499-3524. DOI: 10.1002/hyp.1041.

Monien P, Lettmann KA, Monien D, Asendorf S, Wöfl AC, Lim CH, Thal J, Schnetger B. and Brumsack HJ. 2014. Redox conditions and trace metal cycling in coastal sediments from the maritime Antarctic. *Geochimica et Cosmochimica Acta* **141**: 26-44.

DOI: 10.1016/j.gca.2014.06.003.

Moore RD. 2005. Slug injection using salt in solution. *Watershed Management Bulletin* **8**(2): 1-6.

Nowak, A. and Hodson, A.J. 2013. Hydrological response of a High Arctic catchment to changing climate over the past 35 years; A case study of Bayelva River watershed, Svalbard, *Polar Research* **32**, 19691, <http://dx.doi.org/10.3402/polar.v32i0.19691>.

Nowak A. and Hodson A. 2014a. On the biogeochemical response of a glacierized High Arctic watershed to climate change: Revealing patterns, processes and heterogeneity among micro-catchments. *Hydrological Processes* In Press. DOI: 10.1002/hyp.10263.

Nowak A. and Hodson A. 2014b. Changes in meltwater chemistry over a 20 year period following a thermal regime switch from polythermal to cold-based glaciation at Austre Brøggerbreen, Svalbard. *Polar Research* **33**: 22779. DOI: 10.3402/polar.v33.22779.

- Nuth C, Kohler J, Aas HF, Brandt O, and Hagen JO. 2007. Glacier geometry and elevation changes on Svalbard (1936–90): a baseline dataset. *Annals of Glaciology* **46**(1): 106-116. DOI: <http://dx.doi.org/10.3189/172756407782871440>.
- Poulton SW, and Raiswell R. 2005. Chemical and physical characteristics of iron oxides in riverine and glacial meltwater sediments. *Chemical Geology* **218**(3): 203-221. DOI: [10.1016/j.chemgeo.2005.01.007](https://doi.org/10.1016/j.chemgeo.2005.01.007).
- Raiswell R. 1984. Chemical models of solute acquisition in glacial meltwaters. *Journal of Glaciology* **30**(104): 49-57.
- Raiswell R, and Canfield DE. 2012. The iron biogeochemical cycle past and present. *Geochemical Perspectives* **1**(1), 1-2.
- Raiswell R, Tranter M, Benning LG, Siegert M, De'ath R, Huybrechts P, and Payne T. 2006. Contributions from glacially derived sediment to the global iron (oxyhydr) oxide cycle: Implications for iron delivery to the oceans. *Geochimica et Cosmochimica Acta* **70**(11): 2765-2780. DOI: [10.1016/j.gca.2005.12.027](https://doi.org/10.1016/j.gca.2005.12.027).
- Riber L. 2009. Paleogene depositional conditions and climatic changes of the Frysjaodden Formation in central Spitsbergen (sedimentology and mineralogy). Unpublished University of Oslo MSc thesis, 113 p. <http://urn.nb.no/URN:NBN:no-22636>.
- Rutter N, Hodson A, Irvine-Fynn T, and Solås MK. 2011. Hydrology and hydrochemistry of a deglaciating high-Arctic catchment, Svalbard. *Journal of Hydrology* **410**(1): 39-50. DOI: [10.1016/j.jhydrol.2011.09.001](https://doi.org/10.1016/j.jhydrol.2011.09.001).
- Schroth AW, Crusius J, Chever F, Bostick BC, and Rouxel OJ. 2011. Glacial influence on the geochemistry of riverine iron fluxes to the Gulf of Alaska and effects of deglaciation. *Geophysical Research Letters* **38**(16): DOI: [10.1029/2011GL048367](https://doi.org/10.1029/2011GL048367).
- Schoonen MA. 2004. Mechanisms of sedimentary pyrite formation. *Geological Society of America Special Papers* **379**: 117-134. DOI: [10.1130/0-8137-2379-5.117](https://doi.org/10.1130/0-8137-2379-5.117).
- Statham PJ, Skidmore M, and Tranter M. 2008. Inputs of glacially derived dissolved and colloidal iron to the coastal ocean and implications for primary productivity. *Global Biogeochemical Cycles* **22**(3): GB3013. DOI: [10.1029/2007GB003106](https://doi.org/10.1029/2007GB003106).
- Soltvedt S. 2000. Postglacial sediment transport in Endalen, Svalbard. Cand. Scient. Thesis, Bergen University, 144 pp. [www.ub.uib.no/elpub/2000/h/420001/Hovedoppgave.pdf](http://www.ub.uib.no/elpub/2000/h/420001/Hovedoppgave.pdf).
- Strzelecki MC, Małecki J, and Zagórski P. 2015. The Influence of Recent Deglaciation and Associated Sediment Flux on the Functioning of Polar Coastal Zone–Northern Petuniabukta, Svalbard. In *Sediment Fluxes in Coastal Areas* (pp. 23-45). Springer Netherlands. DOI: [10.1007/978-94-017-9260-8\\_2](https://doi.org/10.1007/978-94-017-9260-8_2).
- Svinth AAG. 2013. A Sedimentological and Petrographical Investigation of the Todalen Member and the Boundary Beds of the Endalen Member within the Firkanten Formation (Paleocene) in the Central Basin of Spitsbergen, Svalbard. Unpublished Masters Thesis, Norwegian University of Science and Technology, Norway, 163 pp. <http://urn.kb.se/resolve?urn=urn:nbn:no:ntnu:diva-23133>.
- Tockner K, Malard F, Uehlinger U, and Ward JV. 2002. Nutrients and organic matter in a glacial river-floodplain system (Val Roseg, Switzerland). *Limnology and Oceanography* **47**(1): 266-277. DOI: [10.4319/lo.2002.47.1.0266](https://doi.org/10.4319/lo.2002.47.1.0266).

Tranter M, Brown GH, Hodson AJ, and Gurnell AM. 1996. Hydrochemistry as an indicator of subglacial drainage system structure: a comparison of alpine and sub-polar environments. *Hydrological Processes* **10** (4), 541-556.

Wadham JL, Cooper RJ, Tranter M, and Bottrell S. 2007. Evidence for widespread anoxia in the proglacial zone of an Arctic glacier. *Chemical Geology* **243**(1): 1-15.

DOI: 10.1002/(SICI)1099-1085(199604)10:4.

Wehrmann LM, Formolo MJ, Owens JD, Raiswell R, Ferdelman TG, Riedinger N, and Lyons TW. 2014. Iron and manganese speciation and cycling in glacially influenced high-latitude fjord sediments (West Spitsbergen, Svalbard): Evidence for a benthic recycling-transport mechanism. *Geochimica et Cosmochimica Acta* **141**, 628-655. DOI: 10.1016/j.gca.2014.06.007.

Wynn PM, Hodson AJ and Heaton T. 2006. Chemical and isotopic switching within the subglacial environment of a High Arctic glacier, *Biogeochemistry* **78**(2), 173-193.

DOI:10.1007/s10533-005-3832-0.

Wynn PM, Hodson AJ, Heaton TH, and Chenery SR. 2007. Nitrate production beneath a High Arctic glacier, Svalbard. *Chemical geology* **244**(1): 88-102.

DOI:10.1016/j.chemgeo.2007.06.008.

Yde, JC, Riger-Kusk M, Christiansen HH, Knudsen NT. and Humlum O. 2008.

Hydrochemical characteristics of bulk meltwater from an entire ablation season, Longyearbreen, Svalbard. *Journal of Glaciology* **54**(185): 259-272. DOI:

10.3189/002214308784886234.

Zhang R, John SG, Zhang J, Ren J, Wu Y, Zhu Z, Sumei L, Xunchi Z, Marsay CM and Wenger, F. 2015. Transport and reaction of iron and iron stable isotopes in glacial meltwaters on Svalbard near Kongsfjorden: From rivers to estuary to ocean. *Earth and Planetary Science Letters* **424**: 201-211. DOI:10.1016/j.epsl.2015.05.031.

Accepted

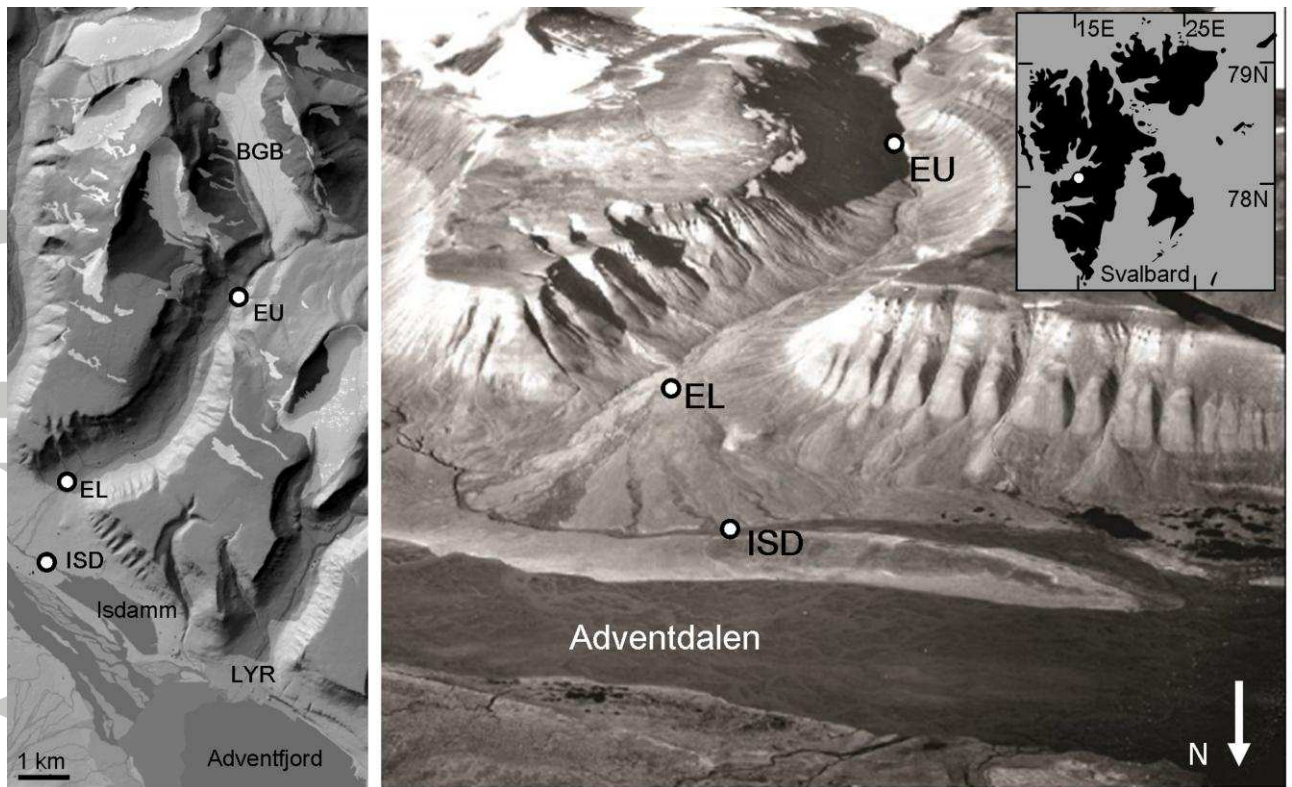


Figure 1. Endalen watershed, showing its intersection with Adventalen and the monitoring sites at Isdammen inflow (ISD); Endalen Lower (EL) and Endalen Upper (EU). “BGB” denotes Bogerbreen, the largest glacier in the valley. “LYR” denotes Longyearbyen. The background photograph is the 1936 oblique aerial photograph (courtesy of the Norwegian Polar Institute).

Accepted

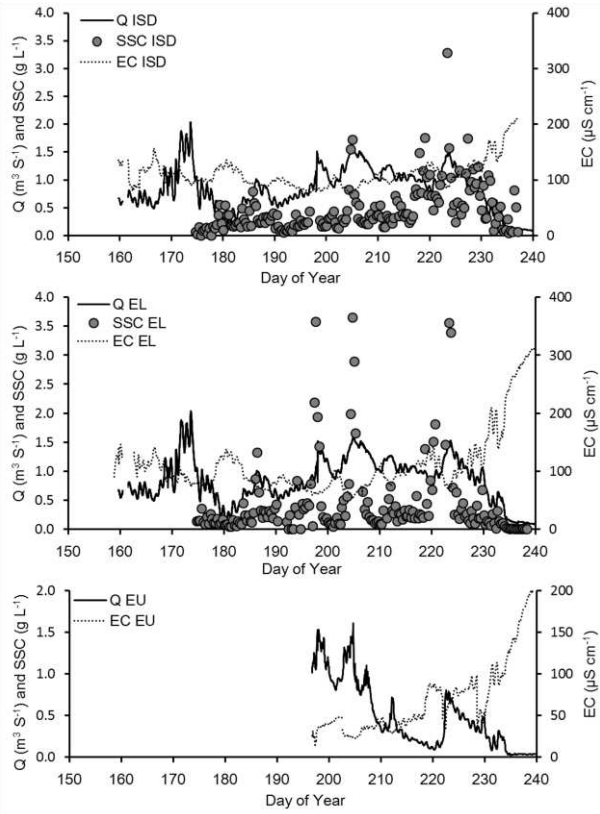


Figure 2. Hourly hydrological time series characteristics at ISD (top), EL (middle) and EU (bottom), including discharge (Q), electrical conductivity (EC) and suspended sediment concentration (SSC).

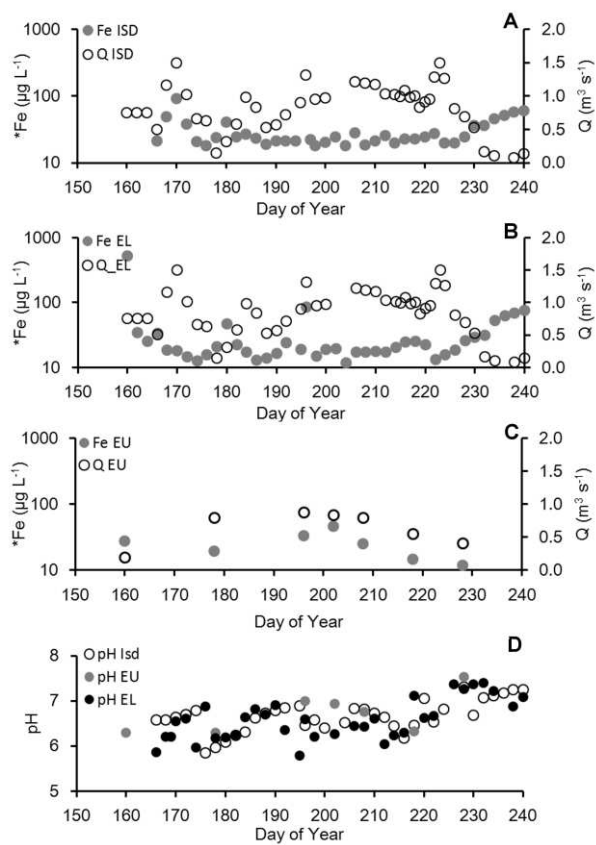


Figure 3. Reactive Iron (\*Fe), discharge (Q) and pH at EU, EL and ISD.

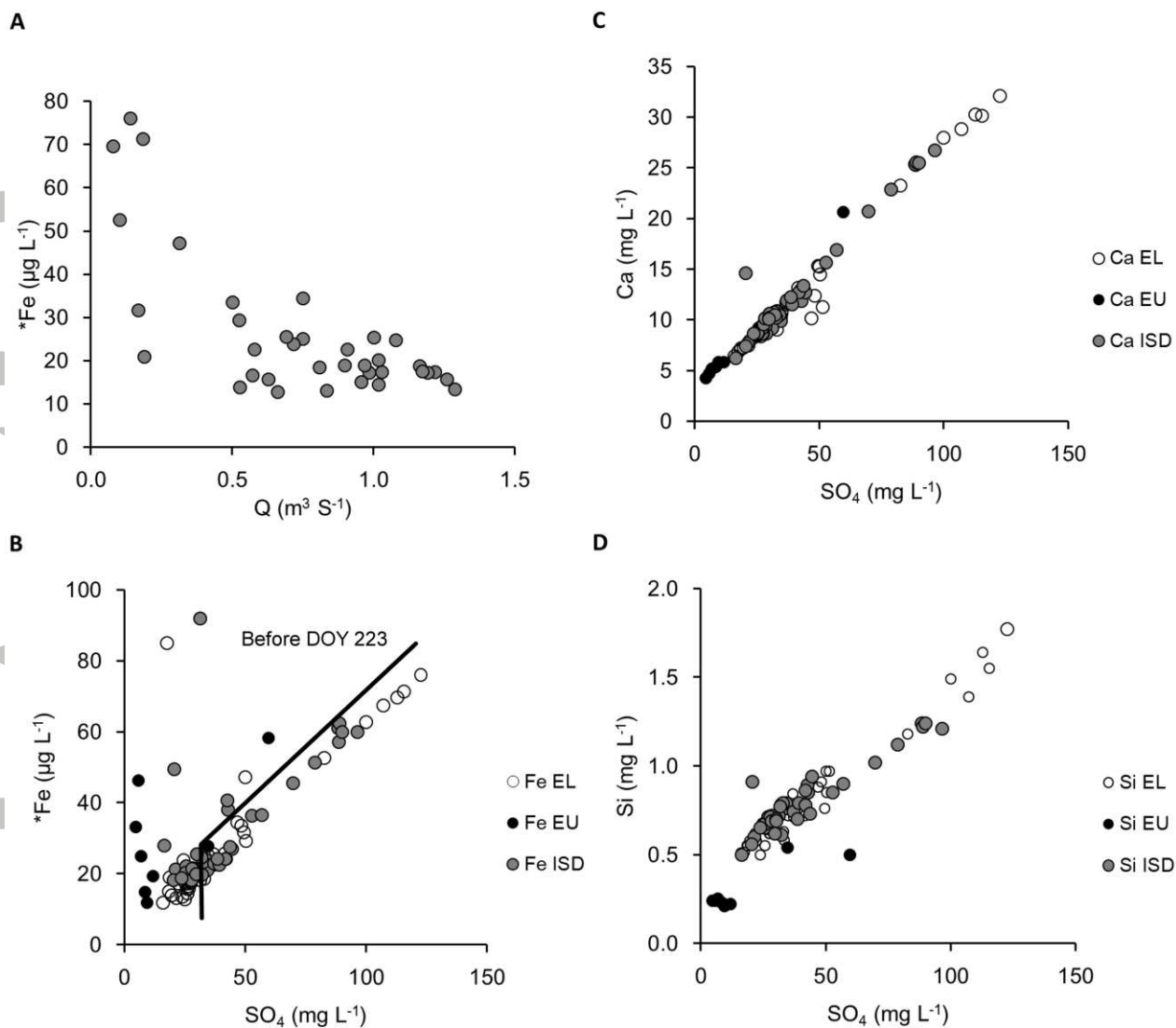


Figure 4. Association between key variables. A) Discharge and \*Fe at Site EL only. B) SO<sub>4</sub><sup>2-</sup> and \*Fe; C) SO<sub>4</sub><sup>2-</sup> and Ca<sup>2+</sup>; D) SO<sub>4</sub><sup>2-</sup> and Si. The solid line in Figure B) separates the data from Sites EL and ISD that were collected before and after DOY 223.

Accepted

Table 1. Details of hydrological monitoring and sampling along the Endalen Valley at the Endalen Upper (EU), Endalen Lower (EL) and Isdammen (Isd) sites.

<b>Parameters</b>	<b>Isd</b>	<b>EL</b>	<b>EU</b>
Hourly runoff, electrical conductivity and water temperature	7 <sup>th</sup> June – 19 <sup>th</sup> August (DOY 159 – 231)	6 <sup>th</sup> June – 29 <sup>th</sup> August (DOY 158 – 241)	14 <sup>th</sup> July – 28 <sup>th</sup> August (DOY 196 – 240)
Suspended sediment monitoring by automatic pump sampler	Three times daily: 22 <sup>nd</sup> June – 25 <sup>th</sup> August (DOY 174 – 237)	Three times daily: 6 <sup>th</sup> June – 25 <sup>th</sup> August	none
Water quality hand sampling	43 samples every other day, 8 <sup>th</sup> June – 29 <sup>th</sup> August (DOY 160 – 241)	43 samples every other day, 8 <sup>th</sup> June – 29 <sup>th</sup> August (DOY 160 – 241)	8 samples weekly, 8 <sup>th</sup> June – 28 <sup>th</sup> August (DOY 160 – 240)

Accepted

Table 2. Runoff, iron and suspended sediment flux (and yield) data for the Endalen Upper (EU), Endalen Lower (EL) and Isdammen (Isd) sites. (<sup>1</sup>The value in parentheses shows the effect of a single, very high iron concentration upon the flow weighted mean concentration. This was not used for the purposes of iron yield estimation).

Site	Area (km <sup>2</sup> )	Qwt Fe (µg/L)	Q (m <sup>3</sup> s <sup>-1</sup> )	Fe flux (kg)	Fe yield (kg km <sup>-2</sup> )	Q (m we.)	SSY (t km <sup>-2</sup> )
<b>DOY 150 - 240</b>							
EL	25.46	22.27 (34.43) <sup>1</sup>	0.86	149	5.85	0.263	136
Isd	28	26.15	0.86	175	6.25	0.239	114
<b>DOY 195 – 240</b>							
EU	9.65	27.3	0.587	62.3	6.45	0.237	n.d.
EL	25.46	24.5	0.903	78.2	3.07	0.138	87.1
Isd	28	23.6	0.903	86.0	2.96	0.125	79.6